Applied Catalysis B: Environmental 136–137 (2013) 334–340

Contents lists available at SciVerse ScienceDirect

Applied Catalysis B: Environmental

journal homepage: www.elsevier.com/locate/apcatb

# A dye-sensitized FeOOH–CNT photocatalyst with three electron transfer channels regulated by hydrogen bonding

Xi-Feng Shi[a,1], Na Li[a,1], Ke Zhao[b], Guan-Wei Cui[a], Ying-Qiang Zhao[a], Ming-Yue Ma[a], Ke-Hua Xu[a], Ping Li[a], Yu-Bin Dong[a,*], Bo Tang[a,*]

[a] College of Chemistry, Chemical Engineering and Materials Science, Engineering Research Center of Pesticide and Medicine Intermediate Clean Production, Ministry of Education, Key Laboratory of Molecular and Nano Probes, Ministry of Education, Shandong Normal University, Jinan 250014, PR China
[b] College of Physics and Electronics, Shandong Normal University, Jinan 250014, PR China

ARTICLE INFO

*Article history:*
Received 16 November 2012
Received in revised form 31 January 2013
Accepted 3 February 2013
Available online 16 February 2013

*Keywords:*
Photocatalysis
Electron transfer
Three channels
Hydrogen bonding

ABSTRACT

A dye-sensitized photocatalyst with three electron transfer channels was constructed, in which FeOOH and photosensitizer $RuL_2Cl_2{\cdot}2H_2O$ were employed as the electron donor, carbon nanotubes were served as the electron container. The catalytic activities of the photocatalyst were evaluated by a model photocatalytic carboxylation reaction of phenol by $CO_2$. The photocatalytic efficiency and transient photocurrent density increased obviously when the catalysis reaction was carried out in cyclohexane compared to two electron activations in water, which suggested the formation of three electron transfer channels in the catalytic system. Moreover, time-dependent density functional theory (TD-DFT) calculation results also indicated the existence of three electron transfer channels assisted by intermolecular hydrogen bonding interaction.



## 1. Introduction

Driven by increasing energy needs and stringent environmental limitations for chemical processes, the search for renewable and clean energy for synthesis chemistry has become a central topic. As an inexpensive, nonpolluting, abundant and renewable natural energy source for performing green chemical reactions, solar light has been widely used in photocatalytic reactions [1–4]. Compared to other types of chemical reactions, photocatalytic reactions have intrinsically advantages in avoiding the generation of toxic substances [5–8].

Recently, many efforts have been made on enhancing the photocatalytic efficiency, of which the efficient separation of electrons and holes is of great importance [9]. It is generally accepted that the formation of electron transfer channels can be in favor of electron transfer, thus enhancing the charge separation and photocatalytic efficiency. When semiconductor photocatalyst, such as $TiO_2$, was solo used in the photochemical reactions, it usually showed quite low photocatalytic activity because of the rapid recombination of conduction band (CB) electrons and valence band (VB) holes [10]. However, the $TiO_2$ decorated with carbon nanotubes (CNTs) [11] could provide one efficient electron transfer channel. As a result, charge recombination was greatly suppressed and high photocatalytic efficiency was obtained by the effective charge transferring from $TiO_2$ to CNT. Further enhancement of the photoelectron transformation efficiency by two electron transfer channels was also reported. These photocatalysts were developed by dye sensitized semiconductor system [12] or hybrid nanostructural materials [13–15]. The results indicated that the photocatalytic efficiency of photocatalysts with two electron transfer channels were better than those with one [16–19]. Hence, it is quite desirable to develop novel photocatalysts with multiple electron transfer channels to investigate the relationship between the number of electron transfer channels and photocatalytic efficiency, which would be beneficial for designing new kind of photocatalysts. To the best of our knowledge, there has been no report on such photocatalysts with three or more electron transfer channels.

$TiO_2$ is an excellent photocatalyst with high activity under UV light conditions. While compared with $TiO_2$, iron oxides such as FeOOH and $Fe_2O_3$ could absorb most of the visible light in the solar spectrum because of its low band gap. It has been reported that iron oxides were observed to be active for the degradation of chlorophenols under visible light, which was comparable with $TiO_2$ [20]. And the more abundant hydroxyl groups on the surface of FeOOH make it easier to be coupled with other components such as dyes and CNT by covalent bonding method, which is advantageous for the construction of multiple electron transfer channels. Herein, we constructed a dye-sensitized FeOOH–carbon nanotubes (FeOOH–CNT) photocatalyst (Fig. 1) with three electron

* Corresponding authors. Fax: +86 531 8618 0017.
*E-mail address:* tangb@sdnu.edu.cn (B. Tang).
[1] These authors contributed equally.

0926-3373/$ – see front matter © 2013 Elsevier B.V. All rights reserved.
http://dx.doi.org/10.1016/j.apcatb.2013.02.005

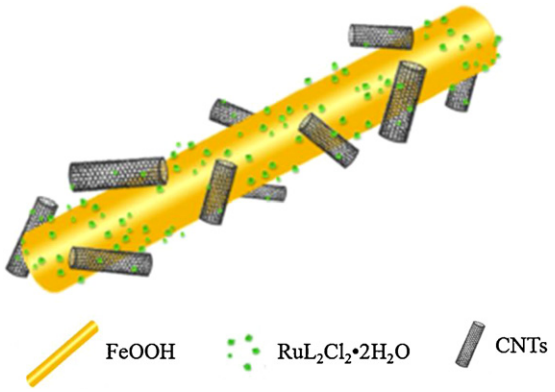


**Fig. 1.** Structure of the $RuL_2Cl_2$–FeOOH–CNT composite.

transfer channels, in which FeOOH rod and the dye $RuL_2Cl_2{\cdot}2H_2O$ (Scheme 1) were employed as the electron donor under visible light, while CNTs were served as the electron container. Inspired by the reported literatures, in which electron transfer channel could be created through hydrogen bonding competition by changing solvents [21–23], the third electron transfer channel can be formed with the assistance of intermolecular hydrogen bonding interaction between $RuL_2Cl_2{\cdot}2H_2O$ and CNT when the photocatalytic reaction was performed in nonpolar solvent, such as cyclohexane. This is the first example of a photocatalyst with three electron transfer channels accomplished by simply changing solvents, which will provide new insights for increasing electron transfer channels and enhancing the photocatalytic efficiency.

## 2. Experimental

### 2.1. Preparation of the catalyst

[$RuL_2Cl_2{\cdot}2H_2O$ (L = 2,2′-bipyridyl-4,4′-dicarboxylic acid)]: The $RuL_2Cl_2{\cdot}2H_2O$ was prepared according to the previous literature [24]. Briefly, $RuCl_3$ (60 mg, 0.229 mol), 2, 2′-bipyridyl-4,4′-dicarboxylic acid (113 mg, 0.463 mol) and 20 mL of dimethylformamide were introduced into a 50-mL flask under constant stirring at 120 °C under the protection of Ar for 8 h. After cooled down to room temperature, the solution was filtrated to remove the insoluble $RuL_3$. Then DMF was removed by vacuum evaporation. The residual solid was recrystallized with acetone and dried at 80 °C for 12 h. The $RuL_2Cl_2{\cdot}2H_2O$ had two crystalliferous water and showed strong absorption at 518 nm and 379 nm in aqueous solution (Fig. S1a).

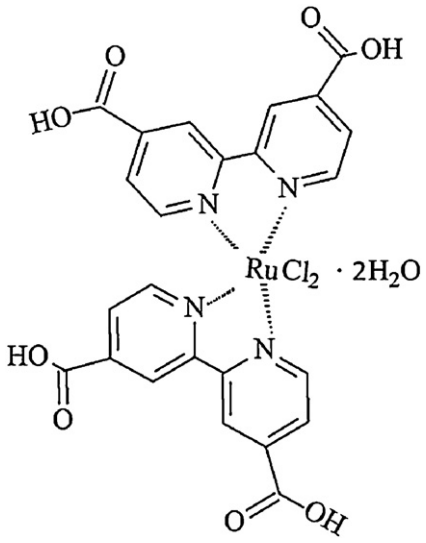


**Scheme 1.** Structure of $RuL_2Cl_2{\cdot}2H_2O$.

[FeOOH]: The preparation of FeOOH nanorods was based on that reported in the literature [25,26]. $FeCl_3$ aqueous solution (4 mL, 0.5 mol/l), $Na_2SO_4$ (0.284 g) and 36 mL of deionized water were introduced into a 50-mL beaker under constant stirring at room temperature for 10 min to give a settled solution. The mixture solution was transferred into a Teflon-lined autoclave of 100 mL capacity. The autoclave was maintained at 140 °C for 12 h and then cooled to room temperature naturally. The resulting solid product was filtered and washed three times with anhydrous ethanol and then dried at 80 °C for 8 h.

[$RuL_2Cl_2$–FeOOH–CNT]: The prepared FeOOH (1.80 g), CNT–COOH (0.39 g), and 80 mL of DMF dried by 4A-zeolite were added into a 100-mL flask under constant stirring at 70 °C for 5 h. Then $RuL_2Cl_2{\cdot}2H_2O$ (0.12 g) was added and continued reacting for 5 h. After cooled down to room temperature, the resulting product was centrifugated, washed with deionized water for three times and dried at 100 °C for 8 h.

### 2.2. Characterization of the catalyst

Thermo gravimetry-differential thermal analyzer (TG-DTA) was performed on TA-SDTQ600 (America) thermogravimetric analyzer, with temperature programming of 10 °C/min from room temperature to 800 °C in $N_2$ atmosphere. Transmission electron microscopy analysis was conducted on a JEM-2100F electron microscope (JEOL, Japan), using a 200 kV accelerating voltage. Infrared spectrum (IR, VERTEX-70, Bruker) analysis was employed to characterize the existence of $RuL_2Cl_2{\cdot}2H_2O$ in the as-synthesized composite. The XPS data were collected in an ultrahigh vacuum chamber equipped with an Al Kα ($h\nu$ = 1486.6 eV) X-ray excitation source by a Thermo Fisher Scientific Escalab 250 X-ray photoelectron spectroscopy. The UV/vis absorption spectrum was measured on a Shimadzu UV-2500 spectrophotometer with $BaSO_4$ powder used as a reference (100% reflectance). The photocatalysis reaction products were detected by HPLC–MS/HPLC (Agilent 1200LC-6520 Q-TOF LC/MS).

### 2.3. Activity tests

The prepared catalyst (30 mg) was ultrasonic dispersed in 30 mL of phenol solution (saturated by $CO_2$) at room temperature. The sample was kept on agitating and bubbling with $CO_2$ in dark for 60 min to allow the adsorption equilibrium. The reactor was then irradiated by a 1000 W Xe lamp with UV cut filters ($\lambda > 420$ nm, 10 cm far away from the photocatalytic reactor). The resulting solution was filtrated and the filtrate was measured by HPLC–MS/HPLC to qualitative and quantitative analysis.

### 2.4. Photoelectrochemical measurements

Photocurrent was measured on an electrochemical analyzer (CHI660D Instruments) in a standard three-electrode system using the prepared samples as the working electrodes with an active area of ca. 2.0 $cm^2$, a Pt sheet as the counter electrode, and saturated calomel electrode as a reference electrode. The working electrodes were prepared as follows: 0.05 g of the sample was grinded with 0.1 g terpinol to make slurry. Then, the slurry was coated onto a 4 cm × 1 cm indium tin oxide-coated glass (ITO glass) electrode by the doctor blade technique. Next, these electrodes were dried in an oven and calcined at 290 °C for 30 min in Ar conditions. All investigated electrodes have a similar film thickness. The electrodes coated with photocatalysts were immersed in required solvents for 48 h respectively. Then the electrode was taken out and immersed

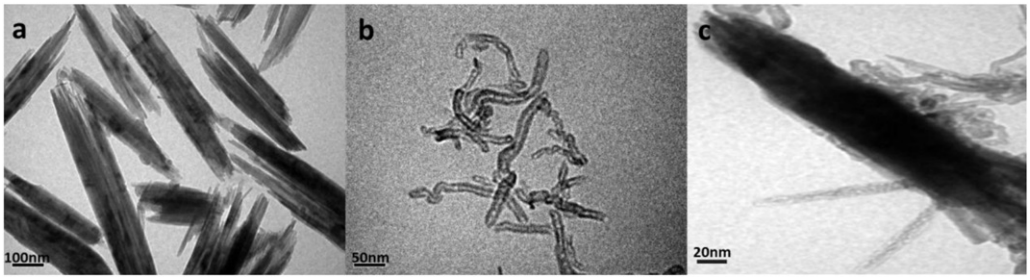


**Fig. 2.** TEM image of (a) FeOOH, (b) CNT and (c) $RuL_2Cl_2$–FeOOH–CNT composite.

in 0.1 M $NaClO_4$ aqueous solution immediately to measure the transient photocurrent. The measurement was carried out under 300 W Xe arc lamp irradiation at 0.6 V/0.4 V vs. saturated calomel electrode.

### 2.5. Theoretical calculations

All calculations were carried out using the Gaussian 03 package [27] at the B3LYP level of theory. The geometry of molecule $RuL_2Cl_2{\cdot}H_2O$ was fully optimized without any constrains. The crystal structure of α-FeOOH was taken from the previous literature [28]. For simplicity, the single-walled (5,5) carbon nanotube (CNT) was considered and the structure was obtained by the Atomistix Virtual Nanolab software [29]. The edges of CNT were ended with hydrogen. The conformations of all the complexes have not been optimized anymore and the geometrical parameters of connection parts were determined artificially. The 6-311 + G basis set was employed for Fe atom. The 6-31G* basis set was used for C, N, O and H atoms, and the 3-21G for Ru and Cl atoms.

## 3. Results and discussion

### 3.1. Characterization of the catalyst

Fig. 2a–c shows the transmission electron microscopy (TEM) images of FeOOH, CNTs and the as prepared $RuL_2Cl_2$–FeOOH–CNT composites. As shown in Fig. 2a and b, FeOOH was a rod with the length of 500–600 nm and the diameter of 50–100 nm, and CNTs were tubes with the length of 150–200 nm and the diameter of 10–20 nm. The TEM images of the resulting $RuL_2Cl_2$–FeOOH–CNT composites (Fig. 2c) indicated the CNTs were supported on FeOOH rods successfully compared with Fig. 2a and b.

Fourier transform infrared spectra (FT-IR) indicated the existence of $RuL_2Cl_2{\cdot}2H_2O$ in the composite. As shown in Fig. S2, the typical absorption peaks of pyridyl ring at 3030 $cm^{-1}$(stretching vibration of C–H), 1569 $cm^{-1}$ and 1628 $cm^{-1}$(skeleton vibration band) were in good agreement with each other in $RuL_2Cl_2{\cdot}2H_2O$ and $RuL_2Cl_2$–FeOOH–CNT. X-ray photoelectron spectroscopy (XPS) indicated that the $RuL_2Cl_2{\cdot}2H_2O$, FeOOH and CNT in $RuL_2Cl_2$–FeOOH–CNT composite were linked by esterification with each other. As shown in Fig. 3, the blue lines were background, the black lines were the results determined by X-ray photoelectron spectroscopy, the red lines were the fitting results using the XPS Peak fitting program and other peaks were the peak resolving results using XPS Acq method. In the high-resolution XPS spectra of $RuL_2Cl_2$–FeOOH–CNT composite, the binding energy of O1s at 529.6 eV of FeO($^*$OH), 532.4 eV of FeO$^*$(OH) and O1s at 530.4 eV of —(CO)O$^*$H, 533.6 eV of —(CO$^*$)OH was in good agreement with the O1s binding energy in FeOOH, CNT–COOH, and $RuL_2Cl_2$ respectively. The typical O1s binding energy value of —(CO)O$^*$— occurred at 531.4 eV in the $RuL_2Cl_2$–FeOOH–CNT composite.

In the UV/vis absorption spectroscopy of $RuL_2Cl_2$–FeOOH–CNT composite (Fig. S3), the absorbance of $RuL_2Cl_2$–FeOOH–CNT was balanced in the full spectrum of 200–800 nm and the fundamental absorption band distinction of FeOOH between UV and visible region was effectively reduced. It might be resulted from the introduction of $RuL_2Cl_2{\cdot}2H_2O$ and CNT, of which the absorption were almost balanced in the entire region of 200–800 nm. The balanced absorbance of $RuL_2Cl_2$–FeOOH–CNT might stabilize the photo absorption which might relatively reduce the electron–hole recombination and enhance the visible light transformation efficiency.

### 3.2. Photocatalysis evaluation and catalysis mechanism

The photocatalysis results suggested 2-hydroxybenzoic acid, 2,2-biphenol and trace benzoic acid (Fig. S4) were formed during the reaction. While in the absence of $CO_2$, biphenyl (Fig. S5) was found, which indicated the existence of $^\bullet C_6H_6$. So the formation of trace benzoic acid could be explained by the existence of $^\bullet C_6H_6$ and $^\bullet$COOH when $CO_2$ was introduced into the photocatalytic reaction. It was reported that it required nearly 2 eV of free energy for one-electron reduction of $CO_2$ to $^\bullet$COOH, which was much higher than that for two-electron reduction of $CO_2$ to HCOOH (0.61 eV) [30–32]. In this case, $CO_2$ might be reduced to HCOOH in the current reaction, which acquired two electrons on the electron trap CNTs, and then HCOOH was oxidized to $^\bullet$COOH by losing one electron to the valence band of FeOOH or the ground state of $RuL_2Cl_2{\cdot}2H_2O$. In addition to the HCOOH electron donor, the phenol could also be oxidized to phenol free radical [33] by losing one electron to the valence band of FeOOH or the ground state of $RuL_2Cl_2{\cdot}2H_2O$. The coexistence of phenol free radical and $^\bullet$COOH resulted in the formation of 2-hydroxybenzoic acid and 2, 2-biphenol. The suggested catalysis reaction mechanism is shown in Fig. 4 and the photocatalytic reaction equation is expressed in Scheme 2.

### 3.3. Activity of the catalyst

To confirm the charge transportation properties and evaluate the photocatalytic efficiency of $RuL_2Cl_2$–FeOOH–CNT, the photocatalytic experiment was performed in different solvents (Fig. 5), and FeOOH–CNT was employed as the reference. As shown in Fig. 5a, there was no distinct difference on the 2-hydroxybenzoic acid evolution of FeOOH–CNT in water and cyclohexane, which was much higher than that of solo FeOOH. The photocatalytic 2-hydroxybenzoic acid evolution of $RuL_2Cl_2$–FeOOH–CNT in water was much higher than that using FeOOH–CNT, while in cyclohexane, the 2-hydroxybenzoic acid evolution of $RuL_2Cl_2$–FeOOH–CNT improved a lot compared with that in water. The reason could be explained as follows: when using FeOOH–CNT as the catalyst, there was only electron transfer channel from FeOOH to CNT, while using $RuL_2Cl_2$–FeOOH–CNT in aqueous solution, there were two electron transfer channels (from $RuL_2Cl_2$ to FeOOH and then to CNT, from FeOOH directly to CNT). In this case, the photoelectron transfer efficiency of the latter was much higher than the former, so the reaction efficiency of the latter was better compared with the former. When

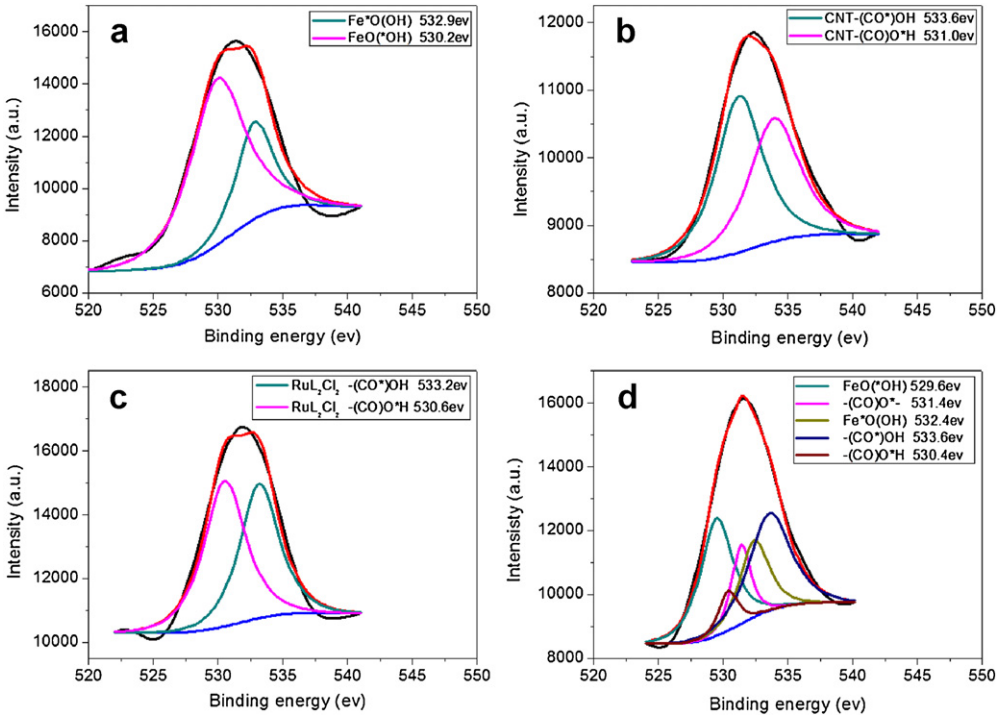


**Fig. 3.** The X-ray photoelectron spectroscopy (XPS) of O1s for (a) FeOOH, (b) CNT, (c) $RuL_2Cl_2{\cdot}2H_2O$ and (d) $RuL_2Cl_2$–FeOOH–CNT composite, respectively. (For interpretation of references to color in this figure legend, the reader is referred to the web version of this article.)

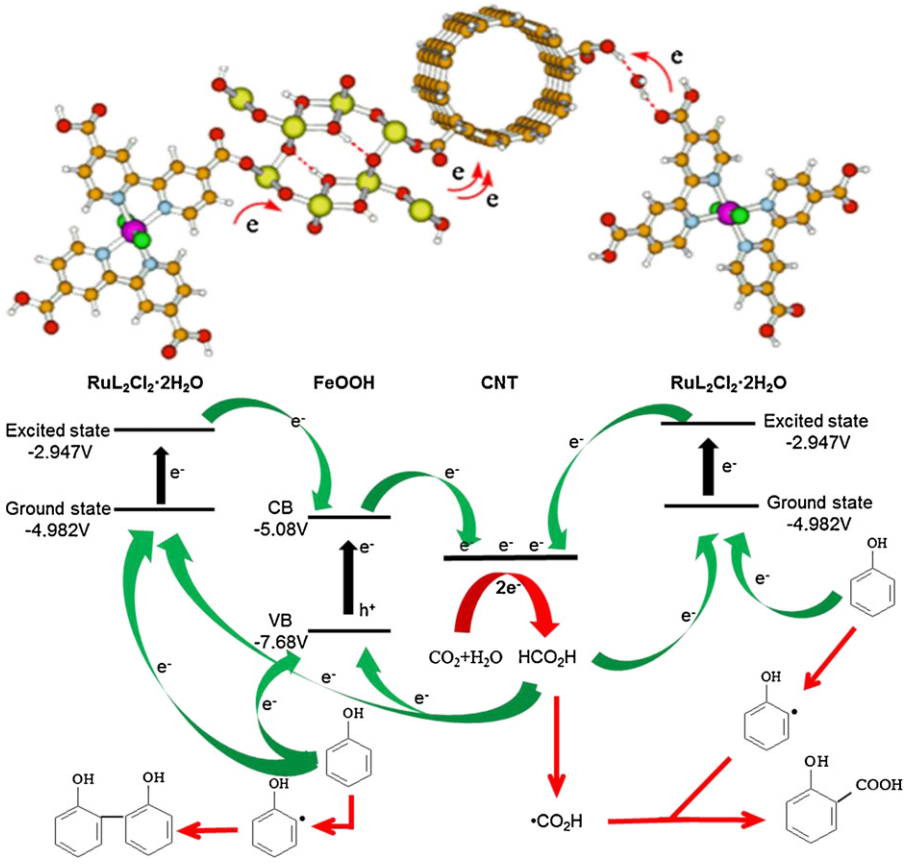


**Fig. 4.** Suggested charge transfer routes and catalytic mechanism of $RuL_2Cl_2$–FeOOH–CNT composite and used in photo induced carboxylation of phenol by $CO_2$.

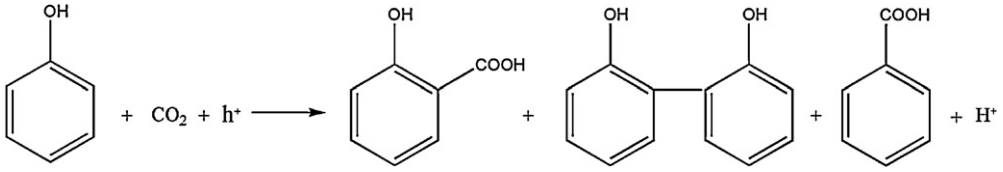


**Scheme 2.** The carboxylation reaction equation of phenol by $CO_2$ photocatalyzed by $RuL_2Cl_2$–FeOOH–CNT composite.

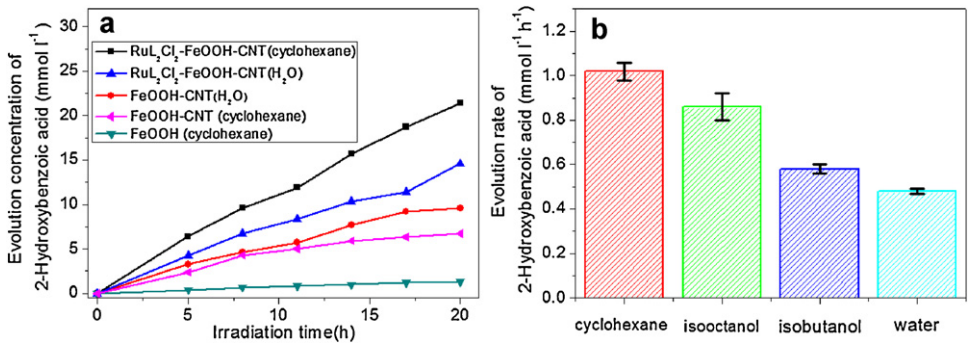


**Fig. 5.** Evolution of 2-hydroxybenzoic acid in photocatalytic system: (a) $RuL_2Cl_2$–FeOOH–CNT in cyclohexane, $RuL_2Cl_2$–FeOOH–CNT in water, FeOOH–CNT in water, FeOOH–CNT in cyclohexane and FeOOH in cyclohexane respectively and (b) $RuL_2Cl_2$–FeOOH–CNT in cyclohexane, isooctanol, isobutanol and water respectively.

cyclohexane was used as the solvent, it was hard to form hydrogen bonding with $RuL_2Cl_2{\cdot}2H_2O$, which was opposite to that in water. For the absence of the solvent competition, $RuL_2Cl_2{\cdot}2H_2O$ was easier to form intermolecular hydrogen bonding with carboxyl CNT, which provide the third electron transfer channel. The results indicated the catalyst with three electron transfer channels ($RuL_2Cl_2$–FeOOH–CNT in cyclohexane) has much better catalytic efficiency than that with two channels ($RuL_2Cl_2$–FeOOH–CNT in water) and one (FeOOH–CNT in water or cyclohexane). And the reaction efficiency of 2-hydroxybenzoic acid evolution catalyzed with three electron transfer channels was 3–10-fold compared with that of the previously reported catalysts (Table 1) [33].

Considering the remarkable influence of solvents on the photocatalytic efficiency, photocatalytic experiments of $RuL_2Cl_2$–FeOOH–CNT in different solvents was carried out. The results in water, isobutanol, isooctanol and cyclohexane respectively indicated a gradually improvement in 2-hydroxybenzoic acid evolution (Fig. 5b). The different catalysis efficiency in the above mentioned solvents might result from the hydrogen bonding strength between $RuL_2Cl_2{\cdot}2H_2O$ and the solvents, which would affect the hydrogen bonding strength between $RuL_2Cl_2{\cdot}2H_2O$ and carboxyl CNT. As the hydrogen bonding strength between $RuL_2Cl_2{\cdot}2H_2O$ and water, isobutanol, isooctanol, cyclohexane was weakened respectively, the hydrogen bonding strength between $RuL_2Cl_2{\cdot}2H_2O$ and carboxyl CNTs (the third electron transfer channel) in water, isobutanol, isooctanol and cyclohexane was strengthened and the electron transfer efficiency would be enhanced synchronously. The results confirmed the formation of the third electron transfer channel was indeed assisted by hydrogen bonding.

**Table 1**
Average 2-hydroxybenzoic acid concentrations per hour and BET specific surface areas of $RuL_2Cl_2$–FeOOH–CNT and FeOOH–CNT compared with photocatalysts reported in literature.

| Catalyst | Surface area/$m^2\ g^{-1}$ | 2-Hydroxybenzoic acid/mmol $L^{-1}\ h^{-1}$ |
|---|---|---|
| $RuL_2Cl_2$–FeOOH–CNT (cyclohexane) | 54.1 | 1.11 |
| $RuL_2Cl_2$–FeOOH–CNT ($H_2O$) | 54.1 | 0.749 |
| Anatase $TiO_2$ (Merck) [33] | 10.5 | 0.371 |
| Pt (2.0 mass%)–$WO_3$ [33] (Carlo Erba, RPE) | 16.4 | 0.118 |
| $TiO_2$ (P25 Degussa) [33] | 44.0 | 0.064 |
| Cu (0.1 mass%)–$TiO_2$ [33] (P25 Degussa) | 50.0 | 0.028 |
| $WO_3$ (Carlo Elba, RPE) [33] | 15.5 | 0.019 |
| Rutile $TiO_2$ (tioxide) [33] | 20 | 0.014 |

### 3.4. Transient photocurrent experiments corresponding to the catalyst activity

Corresponding to the photocatalysis activity, transient photocurrent experiments were performed to further confirm the formation of three electron transfer channels assisted by hydrogen bonding of the current catalyst. When the electrode is irradiated, the photoinduced separation of electron–hole pairs shows up gradually increase photocurrent. A steady-state current is achieved once the charge generation and recombination rates reach equilibrium. More electron–hole pairs and low recombination rates should give rise to long equilibrium time. As can be seen from Fig. 6a, the steady-state current density of FeOOH–CNT (in water), $RuL_2Cl_2$–FeOOH–CNT (in water) and $RuL_2Cl_2$–FeOOH–CNT (in cyclohexane) increased gradually, indicating an increase of electron–hole pairs and decrease of recombination rates in three systems. It suggested that three electron transfer channels were formed for $RuL_2Cl_2$–FeOOH–CNT in cyclohexane. The improved photoelectron separation efficiency was induced by the increase of electron transfer channels. Moreover, transient photocurrent density (Fig. 6b) showed gradually improvement for $RuL_2Cl_2$–FeOOH–CNT in water, isobutanol, isooctanol and cyclohexane, which was in good agreement with the photocatalysis results as expected for the influence of intermolecular hydrogen bonding between $RuL_2Cl_2{\cdot}2H_2O$ and carboxyl CNT.

### 3.5. Age of the catalyst

To assess stability of the photocatalyst in catalytic system, the photo redox experiment was carried out repeatedly six times. As shown in Fig. S6, the catalyst was stable under repeated application with constant reaction rate.

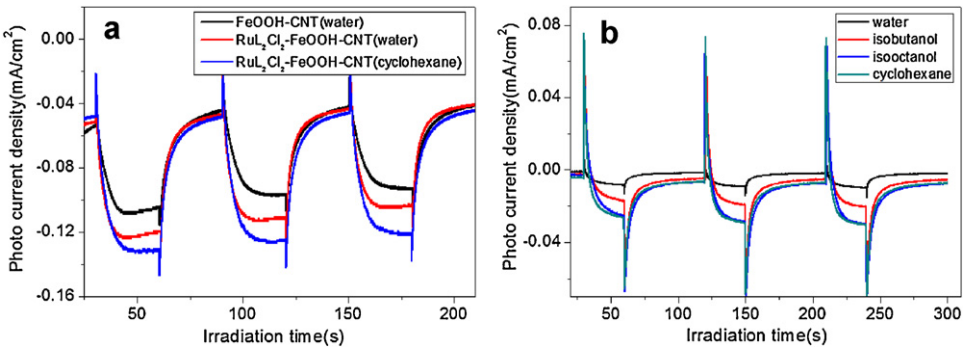


**Fig. 6.** Transient photocurrent responses of (a) FeOOH–CNT immersed in $H_2O$, $RuL_2Cl_2$–FeOOH–CNT immersed in $H_2O$, and $RuL_2Cl_2$–FeOOH–CNT immersed in cyclohexane for 48 h respectively and (b) $RuL_2Cl_2$–FeOOH–CNT after immersed in cyclohexane, isooctanol, isobutanol and water for 48 h respectively.

### *3.6. Theoretical calculation for charge transportation and separation of the catalyst*

CNTs have a large electron storage capacity (one electron for every 32 carbon atoms) [34], which could reduce the electron–hole recombination effectively in semiconductor/CNT composite as an excellent electron trap [35,36]. So in the $RuL_2Cl_2$–FeOOH–CNT composite, the electrons on conduction band of FeOOH separated by CNT provide the first electron transfer channel from FeOOH to CNT. As an explanation for the other two electron transfer channels, the charge transportation and separation under photo irradiation of $RuL_2Cl_2$–FeOOH–CNT was performed by time-dependent density functional theory (TD-DFT) calculation. Fig. 7A illustrated the calculated molecular orbitals (MOs) that were involved in strong electronic excitation of complex $RuL_2Cl_2$–FeOOH. The excitation to the fifth excited state which had considerable oscillator strength, was a result of the transfer from the highest occupied molecular orbital (HOMO) to the lowest unoccupied molecular orbital (LUMO). The MOs displayed the charge transferred from $RuL_2Cl_2{\cdot}2H_2O$ to FeOOH moiety. For a better understanding of the charge transfer (CT) process, we had plotted the charge density difference between the CT state and the ground state, which was visualized by the use of MOLEKEL program [37]. Upon the excitation, the center of molecule $RuL_2Cl_2{\cdot}2H_2O$ lost electron and the place of electron gained only resides on the side of FeOOH moiety. Then the electron transferred to CNTs via FeOOH, which provided the second electron transfer channel.

Considering that there was crystalliferous water in $RuL_2Cl_2{\cdot}2H_2O$ molecule (Fig. S1b), another possible CT channel was proposed, in which the charge could transfer from $RuL_2Cl_2{\cdot}2H_2O$ molecule to CNT directly with the help of hydrogen bonding assisted by the crystalliferous water. To verify the hypothesis, we constructed the complex $RuL_2Cl_2$–$H_2O$–CNT and calculated its CT properties. The results are presented in Fig. 7B). In this case, the HOMO-2 → LUMO transfer were involved in the strong electronic excitation and the MOs (Fig. 7(B)-(a)) did exhibit that the charge transferred from molecule $RuL_2Cl_2{\cdot}2H_2O$ to CNT. Fig. 7(B)-(b) showed large areas of molecule $RuL_2Cl_2{\cdot}2H_2O$ in complex lose electron and the distribution was quite different from the result of single molecule, which was shown in Fig. 7(B)-(c). It demonstrated that the electron could be easier to transfer from center to edge of molecule $RuL_2Cl_2{\cdot}2H_2O$ in complex assisted by intermolecular hydrogen bonding. This was the third electron transfer channel in the current catalyst. The schematic diagram of the electron transfer for $RuL_2Cl_2$–FeOOH–CNT is shown in Fig. 7C. The theoretical calculation results further explained the three electron transfer channels on energy level.

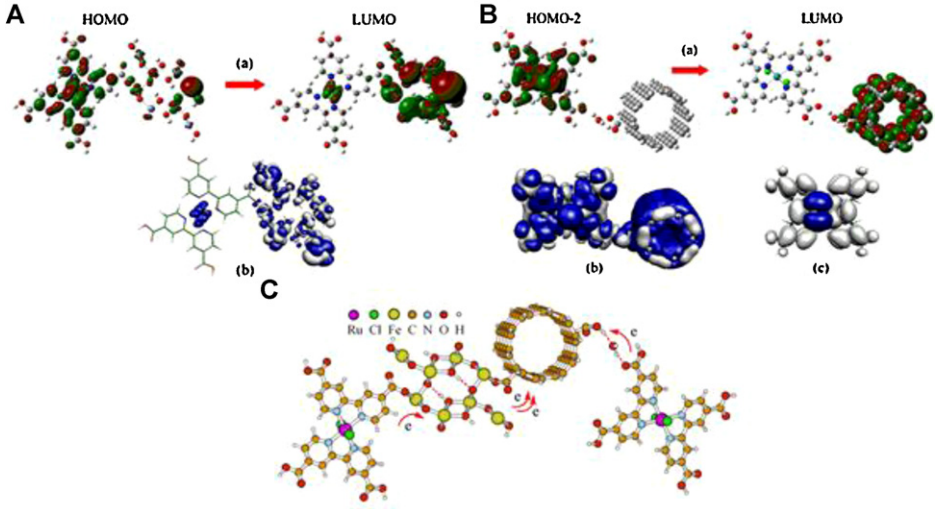


**Fig. 7.** (A) Molecular orbitals (a) that are involved in strong electronic excitation of complex $RuL_2Cl_2$–FeOOH and the charge density difference between the charge transfer state and the ground of complex $RuL_2Cl_2$–FeOOH (b). Areas in white and blue represent the electron gain and loss. (B) Molecular orbitals (a) that are involved in strong electronic excitation of complex $RuL_2Cl_2$–$H_2O$–CNT. The charge density difference between the charge transfer state and the ground of complex $RuL_2Cl_2$–$H_2O$–CNT (b) and molecule $RuL_2Cl_2{\cdot}2H_2O$ (c). Areas in white and blue represent the electron gain and loss. (C) The proposed charge transfer process of $RuL_2Cl_2$ → FeOOH → CNT. (For interpretation of references to color in this figure legend, the reader is referred to the web version of this article.)

## 4. Conclusions

We have demonstrated a visible light catalyst for efficient and clean evolution of 2-hydroxybenzoic acid. The catalyst with three electron transfer channels driven by intermolecular hydrogen bonding, which has never been reported before, performs better photocatalytic efficiency and higher transient photocurrent density than those with one or two channels. Theoretical calculation results further explained the formation of three electron transfer channels driven by intermolecular hydrogen bonding. We anticipate that the current study provides new opportunities for photochemistry to improve photocatalytic efficiency by employing multiple electron transfer channels realized by changing solvents.

## Acknowledgements

This work was supported by 973 Program (2013CB933800), National Natural Science Foundation of China (21035003, 21227005, 21105059, 10904085), Specialized Research Fund for the Doctoral Program of Higher Education of China (20113704130001) and Program for Changjiang Scholars and Innovative Research Team in University.

## Appendix A. Supplementary data

Supplementary data associated with this article can be found, in the online version, at http://dx.doi.org/10.1016/j.apcatb.2013.02.005.

## References

[1] P.Y. Tehshik, A.I. Michael, D. Juana, Nature Chemistry 2 (2010) 527–532.
[2] H. Norbert, Chemical Reviews 108 (2008) 1052–1103.
[3] F. Maurizio, D. Daniele, R. Davide, A. Angelo, Chemical Reviews 107 (2007) 2725–2756.
[4] M.R.N. Jagan, R.J.S. Corey, Chemical Society Reviews 40 (2011) 102–113.
[5] D. Gust, T.A. Moore, Science 244 (1989) 35–41.
[6] T.J. Meyer, Accounts of Chemical Research 22 (1989) 163–170.
[7] D. Gust, T.A. Moore, A.L. Moore, Accounts of Chemical Research 26 (1993) 198–205.
[8] V. Balzani, A. Credi, M. Venturi, ChemSusChem 1 (2008) 26–58.
[9] J.C. Liu, H.W. Bai, Y.J. Wang, Z.Y. Liu, X.W. Zhang, S.D. Darren, Advanced Functional Materials 20 (2010) 4175–4181.
[10] H. Yu, X. Quan, S. Chen, H. Zhao, Y. Zhang, Journal of Photochemistry and Photobiology A: Chemistry 200 (2008) 301–306.
[11] B. Gao, G.Z. Chen, G.L. Puma, Applied Catalysis B: Environmental 89 (2009) 503–509.
[12] M. Zhang, C. Chen, W. Ma, J. Zhao, Angewandte Chemie 120 (2008) 9876–9879.
[13] H. Tada, Q. Jin, H. Nishijima, H. Yamamoto, M. Fujishima, S. Okuoka, T. Hattori, Y. Sumida, H. Kobayashi, Angewandte Chemie International Edition 50 (2011) 3501–3505.
[14] G. Xi, S. Ouyang, J. Ye, Chemistry A European Journal 17 (2011) 9057–9061.
[15] Q. Jin, M. Fujishima, H. Tada, The Journal of Physical Chemistry C 115 (2011) 6478–6483.
[16] W.W. Thomas, S. Sally, R. Erwin, P. Elizabeth, W.R. Stephen, A.A. Fraser, Journal of the American Chemical Society 132 (2010) 2132–2133.
[17] S. Shunsuke, M. Takeshi, S. Shu, K. Tsutomu, M. Tomoyoshi, Angewandte Chemie International Edition 49 (2010) 5101–5105.
[18] W.J. Youngblood, S.H.A. Lee, M. Kazuhiko, T.E. Mallouk, Accounts of Chemical Research 42 (2009) 1966–1973.
[19] U.P. Apfel, W. Weigand, Angewandte Chemie International Edition 50 (2011) 4262–4264.
[20] J. Bandara, J.A. Mielczarski, A. Lopez, J. Kiwi, Applied Catalysis B: Environmental 34 (2001) 321–333.
[21] B.A. Diner, D.A. Force, D.W. Randall, R.D. Britt, Biochemistry 37 (1998) 17931–17943.
[22] K. Hirakawaa, H. Segawab, Journal of Photochemistry and Photobiology A: Chemistry 213 (2010) 73–79.
[23] H.N. Ghosh, K. Adamczyk, S. Verma, J. Dreyer, E.T.J. Nibbering, Chemistry A European Journal 18 (2012) 4930–4937.
[24] P. Liska, N. Vlachopoulos, M.K. Nazeeruddin, P. Comte, M. Gratzel, Journal of the American Chemical Society 110 (1988) 3686–3687.
[25] Z.Z. Sun, X.M. Feng, W.H. Hou, Nanotechnology 18 (2007) 455607–455615.
[26] Y.M. Dong, H.X. Yang, R.C. Rao, A.M. Zhang, Journal of Nanoscience and Nanotechnology 9 (2009) 4774–4779.
[27] Gaussian 03, revision D.01, Gaussian Inc., Wallingford, CT, 2004, http://www.gaussian.com
[28] S.K. Ghose, G.A. Waychunas, T.P. Trainor, P.J. Eng, Geochimica et Cosmochimica Acta 74 (2010) 1943–1953.
[29] Atomistix Virtual Nanolab, Reference in http://www.atomistix.com/
[30] P. Atkins, T. Overton, J. Rourke, M. Weller, F. Armstrong, Inorganic Chemistry, 4th ed., Oxford University Press, Oxford, UK, 2006.
[31] W.H. Koppenol, J.D. Rush, The Journal of Physical Chemistry 91 (1987) 4429–4430.
[32] J. Schneider, H.F. Jia, J.T. Muckerman, E. Fujita, Chemical Society Reviews 41 (2012) 2036–2051.
[33] A. Sclafani, L. Palmisano, G. Farneti, Chemical Communications (1997) 529–530.
[34] A. Kongkanand, P.V. Kamat, ACS Nano 1 (2007) 13–21.
[35] J. Yu, T. Ma, S. Liu, Physical Chemistry Chemical Physics 13 (2011) 3491–3501.
[36] A. Kongkanand, A.M. Domínguez, P.V. Kamat, Nano Letter 7 (2007) 676–680.
[37] MOLEKEL, Reference in http://www.cscs.ch/molekel/